Study on sensitivities of generalized RRI method for data analysis of CSAMT survey

Hee Joon Kim[1], Mi Kyung Park[1] and Soon Jee Seol[1]

[1]Dept. of Environmental Exploration Engineering, PKNU, hjkim@pknu.ac.kr

인공전류원 MT탐사 자료해석을 위한 GRRI법의 감도해석에 관한 연구

김희준, 박미경, 설순지

부경대학교 환경탐사공학과

Abstract: This paper presents sensitivity analysis of generalized rapid relaxation inversion (GRRI) algorithm for inverting controlled-source audio-frequency magnetotelluric (CSAMT) data. The algorithm was originally developed by modifying the RRI algorithm to recover a two-dimensional (2-D) conductivity structure of the Earth from MT data, but can be extended to include CSAMT data if it is combined with 2.5-D forward modeling. These GRRI approximate sensitivities are validated by comparison with exact 1-D and 2.5-D sensitivities. The comparison shows that the GRRI sensitivity is a good approximation to the exact sensitivity and has about half magnitude of the RRI sensitivity. Although the magnitude of the GRRI sensitivity is still slightly larger than that of the 2.5-D sensitivity, both sensitivities are broadly similar in shape when source-receiver offsets are greater than one skin depth on the Earth.
Key words: GRRI, CSAMT, sensitivities, 2.5-D forward modeling

요약: 본 연구는 인공전류원 MT (CSAMT) 자료를 역산하기 위해 GRRI 알고리듬 분석을 실행하였다. 이 알고리듬은 MT 자료로부터 지반의 2차원 전도체 구조를 파악하기 위해 수정 RRI 알고리듬으로부터 독창적으로 개발된 것이나, 2.5차원 전진모델링을 결합시킬 수만 있다면, CSAMT자료까지 해석이 가능하다. 이러한 GRRI 근사감도는 정확한1차원과 2.5차원의 감도와 비교함으로써 그 유용성을 검증할 수 있다. 그 결과, GRRI의 감도는 RRI 감도의 절반 정도이며 전반적으로 2.5차원의 감도와 매우 근사함을 보여준다. 비록 GRRI의 감도크기가 2.5차원의 감도보다 약간 크게 나타나고 있기는 하지만, 송신과 수신의 오프셋이 표피심도 1 보다 큰 경우의 감도는 유사하였다.
주요어: GRRI, 인공전류원 MT, 감도, 2.5차원 전진 모델링

1. INTRODUCTION

Controlled-source audio-frequency magnetotelluric (CSAMT) method is widely used in engineering and environmental geophysics (Zonge and Hughes, 1991). In the far field beyond a distance of approximately four skin depths from the source, electromagnetic (EM) fields can be assumed to be planar (Sandberg and Hohmann, 1982).

Lu et al. (1999) pointed out the main disadvantages of using plane-wave MT inversion to interpret CSAMT data: the horizontal attenuation inherent to the controlled source is not considered in the MT forward modeling, data collected in the transition zone and near field are not utilized, and it is difficult to determine where the far field begins without knowing the electric structure of the Earth. This geometrical complexity has hindered the development of inversion and modeling algorithms for CSAMT data as compared to the MT method, and full potential of this technique has not been exploited.

The rapid relaxation inversion (RRI) is one of the most efficient methods for interpreting MT data, in which sensitivities are approximated from only the cross terms of the horizontal gradient and the inversion part is 1-D (Smith and Booker, 1991). RRI can handle very large 2-D data sets and has been applied to interpretation of many MT data sets (e.g., Unsworth et al., 1999).

In this paper, we examine the applicability of GRRI method to CSAMT inversion. Since approximate sensitivities obviously do not contain all features of the true sensitivities, it will be of great importance to determine when the GRRI sensitivities will be valid and when they will be inaccurate. We discuss how CSAMT data can be inverted using the GRRI method. The derivation of CSAMT sensitivities is essentially identical to that used by Lee et al. (1995) for MT problems. Next, the usefulness of GRRI over simple RRI is presented through sensitivity analysis for simple model

2. CSAMT

CSAMT is a frequency-domain electromagnetic method which uses a grounded dipole or horizontal loop as an artificial source. Given a realistic CSAMT problem, forward modeling for CSAMT inversion requires that EM fields are modeled in 3-D even though the earth conductivity is parameterized in 2-D. Representing 3-D source fields over the 2-D earth is often called the 2.5-D problem.

In this paper, we use a 2.5-D finite-element method (FEM) formulation of Kwon et al. (2002) for the forward modeling and thus sensitivity evaluation. We introduce electric dipole sources into their original formulation for CSAMT modeling. Fig.1 show geometry of a CSAMT survey with TM-mode and TE-mode.

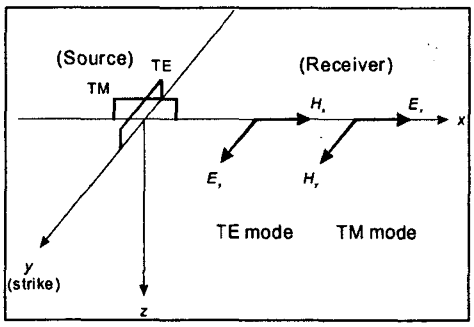

Fig. 1. Geometry of a CSAMT survey.

3. GRRI SCHEME

Let us consider a domain consisting of three vertical columns as shown in Fig. 2. We consider first a case of flat surface, and extend later to a case of terrain surface.

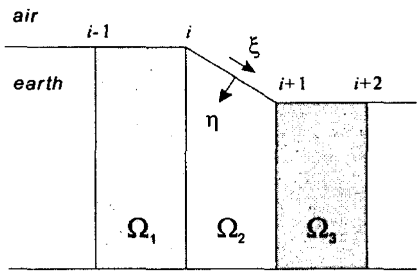

Fig. 2. A domain consisting of three vertical columns with topography.
If the surface of the Earth is flat, the ξ-direction is identical to the x-direction.

The integral in domain Ω_1 can be evaluated since the conductivity variation in that domain has just been calculated through the identical process that started from the left-most column and continues in the positive x-direction. For the evaluation of the integral in domain Ω_3, we can use the conductivity variation obtained and used in the last iteration $\delta\sigma_{k-1}$, where k indicates the k-th iteration.

For completeness, TE-mode GRRI equation is given here. Multiplying equation by test function E^*, which is defined such that H^* is used in the TM-mode scheme, and integrating over the three-column domain yield

$$\iint\left[\frac{\partial^2 \delta E}{\partial x^2}+\frac{\partial^2 \delta E}{\partial z^2}-i\omega\mu\delta(\sigma E)\right]E^* ds = 0\cdot \tag{1}$$

It can be shown that the GRRI scheme is also well suited for inverting data with topography, particularly for TM mode, since the core of the algorithm is not 1-D but 2-D (i.e., the horizontal derivative of magnetic field is used as a part of the functional to be minimized). In the new scheme CSAMT data in the presence of topography the terms will be modified to (Fig. 2)

$$\int_{\xi_{i-1}}^{\xi_{i+2}}\left[\delta\left(\frac{1}{\sigma}\frac{\partial H}{\partial \eta}\right)H^*\right]_{surface} d\xi = \int_{\xi_{i-1}}^{\xi_{i+2}}\left[\delta Z_{\xi y} H H^*\right]_{surface} d\xi\cdot \tag{2}$$

As can be seen in Fig. 2, the surface can be of any topography and the electric fields used are tangential (in the ξ-direction) to the surface. It is consistent with the way that the electric field is measured using an electric dipole.

4. SENSITIVITIES

Most inversions of nonlinear problems require computation of partial derivatives with respect to the parameters of the model. These often appear in the form of the Jacobian

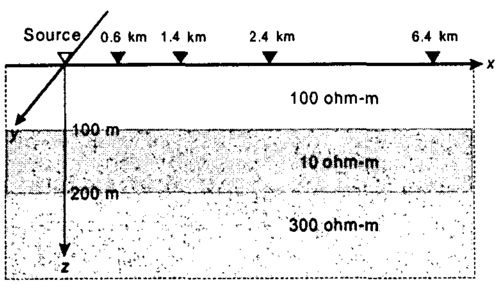

Fig. 3. A collinear array of source and receivers for computing sensitivities over a three-layered half-space.

or sensitivity matrix,

$$J_{ij} = \frac{\partial d_i}{\partial m_j}, \qquad i = 1, \cdots, M, \quad j = 1, \cdots, N, \tag{3}$$

where M and N are the numbers of measurements d_i and model parameters m_j, respectively. Thus, sensitivities quantify how a change in the conductivity of each model cell affects each datum. In this section, approximate sensitivities obtained from the simple RRI and GRRI methods are validated by comparison with the true sensitivities. The models have been used to evaluate the exact sensitivities.

To examine sensitivities in the far field, transition zone and near field, we employ the same models as used in Lu et al. (1999). These are a (1) homogeneous half-space, (2) a three-layered earth with source and receivers on a collinear profile.

Fig. 3 shows the model of the three-layered earth. A source frequency is 64 Hz, and EM fields are picked in either TE or TM mode. Here, the two approximate sensitivities of RRI and GRRI are compared with the other exact ones of 1-D and 2.5-D.

Sensitivities are calculated at four receivers shown in Fig. 3. When the model is the homogeneous half-space of 100 ohm-m, they are approximately positioned at 0.96δ, 2.2δ, 3.8δ, and 10.2δ, respectively, where δ represents the skin depth (about 0.63 km at 64 Hz). The quantities to be compared are $\partial\rho_a/\partial\sigma_i$ and $\partial\phi/\partial\sigma_i$, where ρ_a and ϕ are the apparent resistivity (ohm-m) and impedance phase (°), respectively, and σ_i is the conductivity (S/m) of the ith cell for the exact 2.5-D case or the ith layer of the other cases. The sensitivities are normalized by the vertical thickness of the perturbed cell. In order to compare sensitivities objectively, all comparisons are made in the region with uniform horizontal node spacing in forward modeling.

Fig. 4 shows TE-mode sensitivities on the collinear profile for the homogeneous half-space of 100 ohm-m. Sensitivities decay quickly with depth and are essentially zero below a depth of 1 km (1.6δ). At source-receiver offsets of less than δ, however, not only the magnitudes but also the shapes of 1-D, RRI and GRRI sensitivity curves are quite different from the 2.5-D ones, suggesting that the approximate sensitivities will not be valid in the near field.

Note that both GRRI and 2.5-D sensitivities are broadly similar in shape at source-receiver offsets of greater than δ. This similarity may assure that the sensitivities from the approximate methods are available for inversion of CSAMT data if the model update is adequately scaled. The shape of the sensitivity is most important for guiding inversion in the correct direction. In contrast, the magnitude of the sensitivity has an effect on the step size of the model update. Thus down-seizing the model update is necessary at each inversion iteration, especially at early stages when the model is changing rapidly.

Next, the sensitivities for the three-layered model are shown in Fig. 5 for the same receiver positions used in the homogeneous half-space model. The RRI sensitivity is much greater in magnitude than the 2.5-D sensitivity, and is comparable to the 1-D sensitivity. The GRRI sensitivity, however, has about half magnitude of the RRI sensitivity, and is rather comparable to the 2.5-D sensitivity. Again note that both GRRI and 2.5-D sensitivities are broadly similar in shape, although they have different magnitudes.

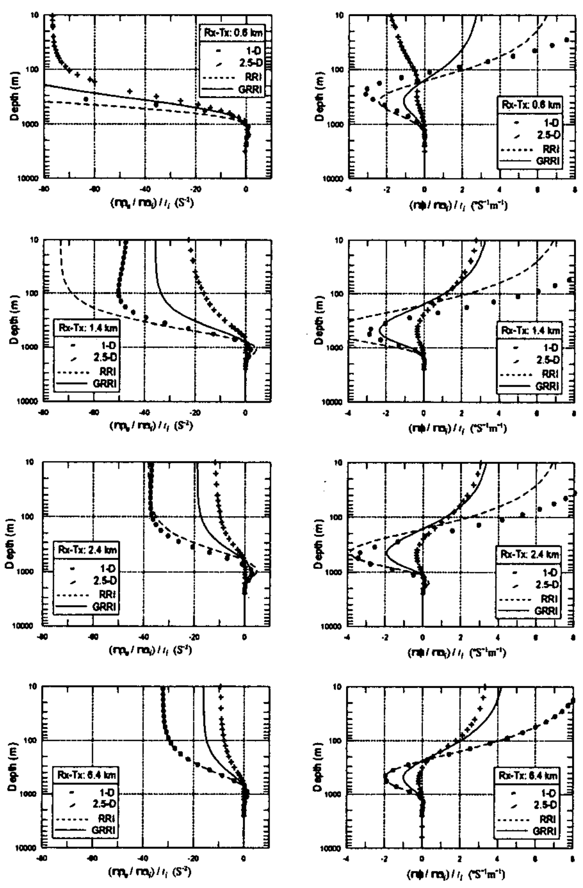

Fig. 4. Normalized sensitivities computed from 1-D analytical, RRI, GRRI, and 2.5-D adjoint-equation methods at the four receivers shown in Fig. 3 over a homogeneous half-space of 100 ohm-m.

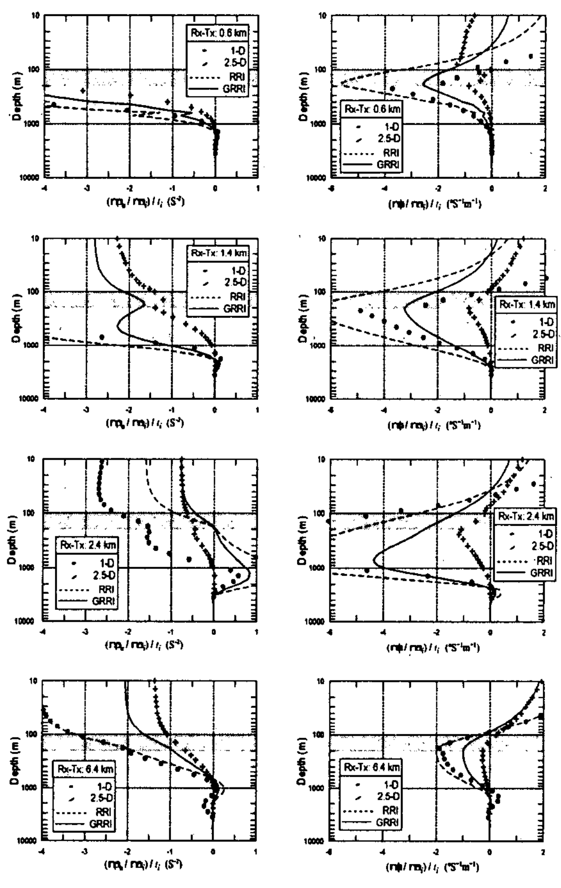

Fig. 5. Normalized sensitivities computed from 1-D analytical, RRI, GRRI, and 2.5-D adjoint-equation methods at the four receivers over the three-layered shown in Fig. 3. Refer to Fig. 4 for units.

Note that the sensitivities in the third layer are greater than in the second layer at some receiver positions. This sensitivity enhancement is quite different from the results form the homogeneous half-space, where the sensitivities decrease monotonically with depth. Also note that the exact 2.5-D sensitivities in the third layer decay to zero quickly below a depth of 1 km, which is about one skin depth in the third layer for 64 Hz.

5. CONCLUSIONS

In this paper, we have examined sensitivities of the GRRI algorithm to see its possibility for inverting CSAMT data. The GRRI algorithm, which was originally developed by modifying the RRI algorithm to recover a 2-D conductivity structure of the Earth from MT data, can be extended to include CSAMT data if it is combined with 2.5-D forward modeling. This algorithm can successfully consider a source effect, which often invalidates the use of conventional MT inversion of CSAMT data. The GRRI approximate sensitivity is validated by comparison with the RRI, 1-D and 2.5-D sensitivities. The comparison shows that the GRRI sensitivity is a good approximation to the exact 2.5-D sensitivity and has about half magnitude of the approximate RRI sensitivity, which is much comparable to the exact 1-D sensitivity. Although the magnitude of GRRI sensitivity is still slightly larger than that of 2.5-D sensitivity, both sensitivities are broadly similar in shape when source-receiver offsets are greater than one skin depth on the Earth. Finally, we can conclude that the GRRI algorithm can be useful to invert CSAMT data gathered in both the transition and far-field zone.

ACKNOWLEDGEMENT: This work was supported by Korea Science and Engineering Foundation (R05−2004−000−12529−0).

REFERENCES

Kwon, H. -S., Song, Y., Son, J. -S., and Suh, J. -H., 2002, 2.5 dimensional EM modeling considering horizontal magnetic dipole source. *Mulli-Tamsa*, **5**, 84-92. (in Korean with English abstract)

Lee, K. H., Xie, G., Yamane, K., and Takasugi, S, 1995, A new 2-D inversion scheme for magnetotelluric data using a modified RRI method. *Proc. World Geothermal Congress*, Florrence, Italy.

Lu, X., Unsworth, M., and Booker, J., 1999, Rapid relaxation inversion of CSAMT data. *Geophys. J. Int.*, **138**, 381−392.

Sandberg, S. K., and Hohmann, G. W., 1982, Controlled-source audiomagnetotellurics in geothermal exploration. *Geophysics*, **59**, 100-116.

Smith, J. T., and Booker, J. R., 1991, Rapid inversion of two- and three-dimensional magnetotelluric data. *J. Geophys. Res.*, **96**, 3905-3922.

Unsworth, M., Egbert, G., and Booker, J., 1999, High resolution electromagnetic imaging of the San Andreas fault in central California. *J. Geophys. Res.*, **104**, 1131-1150.

Zonge, K. L., and Hughes, L. J., 1991, Controlled source audio-frequency magnetotellurics. in Nabighian M. N. ed., Electromagnetic methods in applied geophysics, Vol. 2, B, Soc. *Expl. Geophys.*, Tulsa, 713−809.